RSC Advances

ROYAL SOCIETY OF CHEMISTRY

www.rsc.org/advances

Functionalized mesoporous silica material and anionic dye adsorption: MCM-41 incorporated with amine groups for competitive adsorption of Acid Fuchsine and Acid Orange II

Yunhai Wu[ab*], Meili Zhang[b], Huaiyang Zhao[b], Shengxin Yang[b], Aynigar Arkin[b]

[a] Key Laboratory of Integrated Regulation and Resources Development of Shallow Lakes, Ministry of Education, Hohai University, 1st Xikang Road, Nanjing 210098 (China). Fax: +86-25-83786697; Tel: +86-25-83786697. E-mail: smilehhu@sina.com

[b] College of Environment, Hohai University, 1st Xikang Road, Nanjing 210098 (China).

Abstract

Adsorption of two representative anionic dyes (Acid Fuchsine (AF) and Acid Orange II (AO)) using MCM-41 functionalized with amine groups in the mesoporous silica framework (NH_2-MCM-41) as the adsorbent was investigated. Characterization of the modified adsorbent was studied by BET, FTIR, XRD and SEM. Various parameters including solution pH, adsorbent dosage, contact time, initial dye concentration and temperature were systematically studied. The results showed that the adsorption process was pH dependent, and maximum adsorption capacity for AF was approximately 140.60mg/g at pH 2.0 and 25^{o}C with NH_2-MCM-41 dosage 2.0 g/L, and 278.38mg/g for AO at pH 3.0, respectively. In single component systems, equilibrium data fitted well the Langmuir and D-R models, suggesting the adsorption to be monolayer and physical in nature. Kinetic studies showed that the adsorption

process could be better described by both the Lagergren pseudo-second-order and the Spahn and Schlunder models. Moreover, it was found that the adsorption was governed by film diffusion followed by intraparticle diffusion. Thermodynamic constant values ($\Delta G^o < 0$, $\Delta H^o < 0$ and $\Delta S^o < 0$) demonstrated that the adsorption reactions of AF and AO onto NH_2-MCM-41 were feasible, spontaneous and exothermic under examined conditions. For binary component systems, AF and AO exhibited competitive adsorption onto NH_2-MCM-41, and adsorption capacity values of AF and AO were reduced compared to those of the corresponding single component systems. Furthermore, both in single and binary component systems, the experimental data could be better described by the Langmuir isotherm and the pseudo-second-order kinetic models.

1. Introduction

Dyes are one kind of highly harmful contaminants originating from various industries viz. Paper, textiles, rubber, plastics, cosmetics, leather, food and so on, which pose a worldwide environmental issue due to the inclusion of acids, dissolved solids, toxic compounds, color and possibly harmful heavy metals such as Cr, Ni and Cu[1-5]. Once disposed into the water bodies, dyes not only impart toxicity to the aquatic lives and interfere the balance of water environment, but also cause hazardous influences on human health via damaging vital organs like the brain, kidneys, live and reproductive systems[6-9]. As a consequence, the removal of dyes from industrial effluents is of great significance and should be paid considerable attention.

A great number of conventional methodologies for treating dye-containing wastewaters with varying degrees of advantages have been applied, such as chemical coagulation[10, 11], flocculation[12], oxidation[10, 13, 14], ion exchange[15], irradiation[16, 17], filtration[10, 11, 18], sedimentation[12], solvent extraction[16, 17], reverse osmosis[11], biological treatment[11, 19], photocatalytic degradation[20-22], electrochemical treatment[10, 13, 23] and adsorption[10, 15, 24]. Among the various methods presented above, adsorption process appears to be a successful efficient alternative one in terms of its simplicity, low cost, ease of operation, flexibility, minimum sludge production and insensitivity to specific toxic substances[12, 25, 27].

Adsorption behavior depends heavily on the nature of adsorbent especially its porosity and surface areas[28, 29]. The commonly used adsorbents for dye removal include activated carbon, naturally occurring materials (i.e., clay, gypsum and bentonite), synthetic polymer (i.e., cyclodextrin), agrowaste materials (i.e., sawdust, wood and rice husk), industrial waste (i.e., carbon nanotubes, fly ash and sludge), activated carbon from agrowaste materials (i.e., coconut shell, rice husk and cassava peel), biosorbents (i.e., Aspergillus niger and Spirodela polyrrhiza)[17].

In the past two decades, the ordered mesoporous silica structures have been proposed as the dye adsorbents[30]. Derivatization with organofunctional groups (i.e., amino, diamino, triamino, malonamide, carboxyl, dithiocarbamate, humic acid and imidazole) to the mesoporous silica surface provides easy access to modulate their properties so as to suit those of adsorbates or achieve specific purposes, which has attracted much attention as promising adsorbents to enhance the binding affinity of

dye molecules[31-33]. Recently, a series of amine-functionalized mesoporous materials with large surface area, highly ordered structure and controlled pore diameter were synthesized[34]. Besides, amine-functionalized MCM-41 has been successfully employed to eliminate traces of toxic heavy metal from wastewater[35, 36].

Thus the present work was devoted to researching the ability to remove the organic anionic dye molecules containing sulfonic groups via the application of the modified mesoporous silica material MCM-41. And our purpose was to investigate the adsorption behavior of two basic anionic dyes namely Acid Fuchsine (AF) and Acid Orange II (AO) in aqueous solutions by synthesizing MCM-41 incorporated with amine groups (NH_2-MCM-41) as the adsorbent and evaluate the effects of some independent parameters (solution pH, adsorbent dosage, contact time, initial dye concentration and temperature) on adsorptive removal performance. In addition, the equilibrium isotherms, adsorption kinetics and thermodynamics were analyzed to determine the adsorption mechanism. Besides, the binary dye adsorption investigation was conducted and was modelled with some empirical adsorption isotherm and kinetic models as well.

2. Materials and methods

2.1 Reagents

Two basic anionic dyes with sulfonic groups, namely Acid Fuchsine (AF) and Acid Orange II (AO) were selected as adsorbates to discuss the adsorption performance using the adsorbent MCM-41 which is incorporated with amine groups

(NH_2-MCM-41) in the aspects of porous structure of the adsorbent and the molecular shape of the adsorbates. And the anionic dye compounds were of analytical grade and were used as commercial salts from Nanjing Ruitai Chemical Reagent Co., Ltd. of China, without further purification. Molecular structures of the two dyes are illustrated in Fig. S1 (ESI). Different aqueous solutions of the dyes were prepared by dissolving them in distilled water. A Shimadzu UV-1201 Spectrophotometer and the corresponding calibration curves were adopted to determine the residual concentrations of each dye in aqueous solutions (For AO: λ_{max} =486nm; for AF: λ_{max} =524nm).

2.2 Preparation and characterization of the adsorbents

The mesoporous MCM-41 powder used in the present work was synthesized referring to the literature of Chung-Kung Lee[37], and the final synthesis gel containing a molar composition ratio of CTABr/Na_2O/SiO_2/H_2SO_4/H_2O=1.0:1.76/6.14:1.07/335.23 was treated by stirring, crystallization, filtration, washing, drying and calcification for removing the CTABr in sequence[37]. The preparation method of amine-functionalized MCM-41 (NH_2-MCM-41) was on the basis of the previous literature[35]. 2.5 g of calcined MCM-41 and 2.5 g of 3-aminopropyltrimethoxisilane were both added into a flask containing 50 mL n-hexane and then congealed for 6 hours at room temperature. Afterwards, the NH_2-MCM-41 powder was filtered, washed with 20 mL n-hexane, dried at 105 ^oC for one day, cooled at room temperature overnight, and then stored in an air-tight container, subsequently.

The obtained NH_2-MCM-41 adsorbent was characterized by using different methods. The Quantachrome Autosorb-I Physical Model was used to determine the Brunauer-Emmett-Teller (BET, MICROMERITICS, ASAP 2010, USA) surface area, total pore volume and mean pore radius. Besides, the surface morphology of MCM-41 before and after amine functionazation was visualized by an Scanning Electron Microscopy (SEM, JEOL, JSM-5600V, Japan), which enables the direct observation of the changes in the microstructures of the adsorbents' surface due to the modification process. In order to find out whether -NH_2 had been grafted on MCM-41 successfully, an Fourier Transform Infrared Spectroscopy (FTIR, JASCO 5300) was employed to observe qualitative identification of functional groups on the surface of modified adsorbent, the spectra of which were at the range of 500-4000 cm^{-1} wavenumber. Powder X-ray diffraction (XRD) measurements for the adsorbent before and after modification as well as adsorption were performed with an X-ray diffractometer (ARL Corporation, Switzerland) instrument using Cu $K\alpha$ radiation at 40 kV and 40 mA in the 2θ range 0–50^o.

2.3 Adsorption experiments

The effect of pH was investigated by adding 0.1g NH_2-MCM-41 respectively into two 250mL flasks containing 100mL AF and AO severally, both concentrations of the two dye aqueous solutions were 100mg/L. The pH of the solution was adjusted with 0.1 M HCl or 0.1 M NaOH solutions to the range of 2.0-10.0. Then the tightly stopped flasks were put on temperature-controlled shaker at 180 rpm/min and 25 ^{o}C for 4 hours.

Then samples were collected, filtered and measured.

The impact of adsorbent dosage on adsorption, at the optimum pH (AF: 3.0, AO: 2.0), was determined by adding adsorbent in the range of 0.05-0.5g. After being agitated on a shaker at 180rpm/min and 25 ^{o}C for 4 hours, samples were filtered and analysed.

Moreover, samples collected at 30, 60, 120, 180, 240 and 300min respectively were measured so as to explore the influence of contact time on adsorption. And the effect of the initial dye concentration was conducted by diluting each dye solution of 300mg/L into 20, 50, 100, 150, 200 and 250mg/L separately.

For the binary component systems, the experiments were conducted at the conditions of 25 ^{o}C, pH 2.0 and NH_2-MCM-41 dosage 2.0 g/L. As to the adsorption isotherms, initial concentrations of the dyes were within the range of 100-300mg/L, and samples were filtered and measured after 4 hours. And for the kinetic study, the initial concentration and volume of both the two dyes were respectively 100mg/L and 50mL, and samples were collected and analysed at 30，60，120，180，240，300，360min in sequence.

The adsorptive removal efficiency (η) was determined according to the following equation:

$$\eta = \frac{C_0 - C_e}{C_0} \times 100\% \quad (1)$$

Dyes uptake (q_e) was calculated by the equation as below:

$$q_e = \frac{(C_0 - C_e)}{M} V \quad (2)$$

In addition, all the other chemicals used in this work were of analytical grade.

And the data were the mean values of two replicate determinations. All glassware were cleaned several times and rinsed with distilled water.

3. Results and discussion

3.1 Characterization of the adsorbents

3.1.1 BET surface area, total pore volume and mean pore radius

The BET surface area, total pore volume and mean pore radius of the pure MCM-41 were 921 m^2/g, 0.94 cm^3/g and 3.02nm respectively. For the prepared NH_2-MCM-41, they were 658 m^2/g, 0.75 cm^3/g and 2.71nm respectively, as determined from nitrogen adsorption-desorption isotherms measured at -195 ^oC by the Quantachrome Autosorb-I Physical Adsorption Model. As seen from the data above, the BET surface area, total pore volume and mean pore radius all decreased after amine-functionalization, indicating the successful grafting of -NH_2 groups on the pores of MCM-41.

3.1.2 Scanning electron microscopy

The scanning electron microscopy (SEM) was used to observe the surface morphology of MCM-41 and NH_2-MCM-41. Fig. S2 (ESI) clearly shows that both the surfaces of the two-kind sorbents are rather rough and porous, suggesting the surface structure and stability of MCM-41 were not changed apparently after amine functionalization.

3.1.3 The FTIR spectroscopic analysis

The FTIR spectroscopic analysis was applied to observe qualitative identification of functional groups on the surface of MCM-41 before and after amine functionalization, as well as the adsorption process of AF and AO. Fig. 1 shows the FTIR spectra of MCM-41, NH_2-MCM-41, NH_2-MCM-41-AF and NH_2-MCM-41-AO. A strong and broad band (3250-3750 cm^{-1}) with peaks appeared at 3429 cm^{-1}, which might be attributed to the O-H stretching bonds of silanol groups. The vibrations of Si-O-Si could be seen at 1078 cm^{-1} (asymmetric stretching) and 793 cm^{-1} (symmetric stretching)[38, 39].

After amine fuctionalization, two adsorption peaks at 2936 cm^{-1} and 1562 cm^{-1} occurred, demonstrating that -NH_2 groups had been already grafted on the surface of MCM-41, in agreement with the results of 3.1.1. Moreover, the peaks around 3445 cm^{-1} and 1635 cm^{-1} decreased, which depicts that most O-H stretching bonds were replaced with -CH_2 groups. After AF and AO loading onto NH_2-MCM-41, the FTIR spectrum showed that no visible change except a fluctuant increase appeared in the range of 1250-1750 cm^{-1}, which could be ascribed to the bending vibrations of adsorbed water molecules and N-H groups, suggesting the maintain of relatively intact stability of the mesoporous NH_2-MCM-41 after adsorbing AF and AO dye molecules.

3.1.4 The powder XRD analysis

The powder XRD patterns of MCM-41 before and after the amine modification

accompanied with adsorption of the two anionic dyes onto NH_2-MCM-41 are presented (Fig. S3, ESI), demonstrating a strong diffraction peak in the low-angle region (2θ=1-3^o) for MCM-41 both before and after amine functionalization, which could be related to the mesoporous hexagonal structure of the outer shell, further confirming that the fuctionalization did not change the framework integrity of the mesoporous ordered silica material MCM-41. Besides, the pure MCM-41 illustrated a strong peak and a proportional peak intensities (Fig. S3 a, ESI), whereas the peak of NH_2-MCM-41 was preserved with the disappearance of the other peaks, which might be resulted from the impregnation of amine groups inside the porous channels of MCM-41[40]. In addition, a severe functionalization with amine groups of the phase mesoporous structure appears after adsorption of the two anionic dyes (Fig. S3 b, ESI). And it can be clearly noticed that the adsorption of AF and AO has induced a serious disorder in the porous structure of NH_2-MCM-41[37].

3.2 Adsorption in single component systems

3.2.1 Adsorptive removal behavior of anionic dyes on MCM-41 and NH_2-MCM-41

To enhance Acid Fuchsine (AF) and Acid Orange II (AO) uptake onto the modified MCM-41 is one of the most vital objectives pursued in this present work. AF and AO were selected as the model removal targets, since they are usually ubiquitous in anionic dyeing wastewater. Significant differences existed in the adsorption of AF and AO before and after amine functionalization (Fig. S4, ESI). The removal ratios of AF

and AO by using NH_2-MCM-41 were up to 62.81% and 66.79% respectively, however just 11.85% and 6.60% respectively under the impact of MCM-41, indicating that NH_2-MCM-41 had a higher adsorption capacity to anionic dyes than MCM-41. Resulting from that there were many Si-O and Si-O-H groups on MCM-41, the surface charge became negative so as to adsorb dyes positively charged easily[41]. Besides, comparisons of the maximum adsorption capacities of anionic dyes with various adsorbents which were studied previously and in the present work are listed in Table 1.

Among the numerous different modification methods of MCM-41 aiming to enhance adsorption capacity and selectivity to some specific contaminants, surface functionalization may be quite an effective way that makes great use of the special interaction between the adsorbents and adsorbates[48, 49]. Hence, it is that necessary and meaningful to remove anionic dyes using amine functionalization MCM-41 in this work.

Table 1 Comparisons of the maximum adsorption capacities of anionic dyes on various adsorbents

Adsorbent	Anionic dye	pH	Temperature (^oC)	Maximum adsorption capacity (mg/g)	References
Guava seed carbon	Acid Orange 7	6.0	25	0.63	42
Guava seed carbon	Acid Orange 8	6.0	25	0.91	42
Guava seed carbon	Acid Orange 10	6.0	25	0.10	42
Guava seed carbon	Acid Red 1	6.0	25	0.33	42
Guava seed carbon	Acid blue 80	6.0	25	1.13	42
Guava seed carbon	Acid blue 324	6.0	25	1.09	42
Guava seed carbon	Acid Green 25	6.0	25	1.16	42
Guava seed carbon	Acid Green 27	6.0	25	1.32	42
Mixture almond shells	Direct Red 80	6.0	20±1	22.422	43
Powderred peanut hull	Sunset Yellow	2.0	20±2	13.99	44
Powderred peanut hull	Amaranth	2.0	20±2	14.90	44
Powderred peanut hull	Fast Green FCF	2.0	20±2	15.60	44

Coir pith activated carbon	Reactive Orange 12	3.0	20	16.67	45
Coir pith activated carbon	Reactive Red 12	3.0	20	16.67	45
Coir pith activated carbon	Congo Red	6.0	23	6.107	46
Fungus Aspergillus niger	Congo Red	6.0	23	14.72	47
MCM-41	Acid Red 1	5.0	25	0.6×10^{-4}	37
MCM-41	Erioglaucine	2.0	25	1.0×10^{-4}	37
Al-MCM-41	Acid Yellow 49	10.0	24	46.00	33
NH_2-MCM-41	Acid Fuchsine	3.0	25	140.60	Present study
NH_2-MCM-41	Acid Orange II	2.0	25	278.38	Present study

3.2.2 Effect of solution pH

The adsorptive removal of adsorbates during the adsorption process mainly depends on solution pH, since it affects both the ionization degree and surface property of the adsorbents[50]. As shown in Fig. 2, the removal ratio as well as adsorption capacity decreased rapidly with the increase of solution pH. Under the acidic condition of pH 3.0, the peak removal ratio and maximum capacity of AF adsorption were up to 92.00% and 92.02 mg/g respectively. For AO adsorption, the peak removal ratio (93.86%) and maximum adsorption capacity (93.86 mg/g) occurred at pH 2.0. Nevertheless, under the alkaline condition of pH 10.0, the removal ratios of AF and AO dropped sharply to just 51.37% and 67.91% respectively.

In aqueous solution, sulfonate groups in anionic dyes dissociated and transferred into $-SO_3^-$. Besides, a lot of hydrogen ions existed in solutions of low pH, resulting in that the surface of NH_2-MCM-41 became positively charged ($-NH_3^+$) due to protonation. Then the protonated NH_2-MCM-41 adsorbed a large number of negatively charged anionic dyes in the solution as a result of electrostatic attraction. As pH increased, the available adsorption sites positively charged on the surface of NH_2-MCM-41 decreased subsequently. Meanwhile, sites negatively charged on the

surface of adsorbents became more and more, leading to that much less anionic dyes molecules were adsorbed onto adsorbent on account of electrostatic repulsion. Simultaneously, a large amount of hydroxide ions existed in alkaline aqueous solution, inducing the competitive behavior for available adsorption sites, in accordance with Anbia M and Salehi S[51].

Electrostatic attraction is the primary mechanism during the adsorption process of AF and AO onto NH_2-MCM-41. The dissociation of anionic dyes molecules and their combination with NH_2-MCM-41 in acid medium are proposed in Fig. 3.

3.2.3 Effect of adsorbent dosage

Adsorbent dosage is a vital parameter for measuring the adsorption capacity and removal ratio, since the amount of it added into the solution determined the quantity of binding sites available for adsorption[2, 30]. From Fig. 4, we can see the effect of NH_2-MCM-41 dosage on adsorptive removal ratio of the anionic dyes. It is evident from Fig. 4 that both the removal ratios of AF and AO increased significantly when NH_2-MCM-41 dosage varied from 0.5 g/L to 2.0 g/L. However the ratios increased slowly as the adsorbent dosage increased from 2.0 g/L to 5.0 g/L. Thus 2.0 g/L was chosen as the optimal NH_2-MCM-41 dosage in this study.

More adsorbent dosage into the solution renders larger adsorptive contacting surface area between the adsorbent and adsorbates as well as more active adsorption sites for the anionic dye molecules, therefore resulting in higher adsorptive removal ratio. With other conditions unchanged, increasing adsorbent dosage appropriately

may benefit the adsorptive removal efficiency of contaminants[52, 53].

3.2.4 Effect of contact time

The equilibrium time between the adsorbent and adsorbates is of great importance in the applications of economical adsorption wastewater treatment systems. It is quite necessary to adsorb the target pollutants and reach the equilibrium in a short time for any kind of highly effective adsorbents used in textile industry effluent treatment. As shown in Fig. 5, both the removal ratio and adsorption capacity increased with the increasing contact time, and the increasing velocities of the two dye adsorption process were fast in the initial 240 min. Afterwards, the removal ratio and adsorption capacity became steady and almost changed no longer (AF: 90.38%, 45.19 mg/g; AO: 94.37%, 47.18 mg/g). Therefore, the optimum contact time was selected as 240 min in this work.

During the initial adsorption process, vast adsorbents existed in the aqueous solution, boosting the adsorption rate greatly. However, the adsorption rates dropped afterwards, which could be attributed to the electrostatic repulsion between the two anionic dyes adsorbed on the surface of NH_2-MCM-41 and the remaining dyes with the same negative charge in the aqueous solution. Furthermore, when surface available sites of the adsorbent had been mostly covered with the anionic dyes, the diffusion rate of dye molecules into inner space of NH_2-MCM-41 became slower, leading to a limit of the extent of adsorption.

3.2.5 Effect of initial anionic dye concentration

Fig. 6 represents the effect of initial dye concentration on adsorption of anionic dyes at pH 2.0 for AF and pH 3.0 for AO. It can be observed that the adsorption capacity increased from 23.13 mg/g to 128.50 mg/g for AF and 23.92 mg/g to 136.02 mg/g for AO respectively as the initial concentrations of the two anionic dyes both increased form 50 mg/L to 300 mg/L. The initial concentration of anionic dyes can serve as an essential driving force for overcoming the mass transfer resistance of dye molecules between the aqueous solution and solid-phase adsorbent. As the initial concentrations of AF and AO increased, the driving force became higher as well, which facilitated more dye molecules adsorbed onto the adsorbent NH_2-MCM-41, contributing to better adsorptive removal performance and higher adsorption capacity.

Whereas the data showed that the percentages of adsorptive removal dropped from 92.54% to 85.67% for AF, and 95.64% to 77.67% for AO despite of the increasing adsorption density, which could be explained on the basis of the quantity limit of available active sites on the adsorbent surface. Since a given mass of the adsorbent could just adsorb a finite amount of target dye molecules, the more adsorbent in the effluent, the smaller is the extent of adsorbates that a fixed mass of adsorbent can purify[2].

In consequence, adequate adsorption sites exist at the concentration of relatively low initial dyes. On the contrary, when the concentration of adsorbate is too high, need of "parking space" for dye molecules exceeded the supply of adsorption sites on NH_2-MCM-41 adsorbent, thus causing drop of the adsorptive removal efficiency[54].

3.2.6 Equilibrium isotherms

When the adsorption system is at the state of equilibrium, the distribution of anionic dyes between the liquid phase and adsorbent is obviously vital to establish, which can be generally expressed via one or more of a series of isotherm models[2, 55, 56]. For the present work, the adsorption isotherms used were the Langmuir, Freundlich and Dubinin-Radushkevich (D-R) models, for describing the relationship between the amount of adsorbate adsorbed on adsorbents at equilibrium and the concentration of the remaining anionic dyes in aqueous solution at different temperatures.

The Langmuir model is valid for monolayer adsorption onto the surface of adsorbents containing a finite number of identical sites[57], and the linear form of the isotherm can be expressed by the following equation:

$$\frac{C_e}{q_e} = \frac{C_e}{q_m} + \frac{1}{K_L q_m} \quad (3)$$

The empirical Freundlich model gives an expression encompassing the surface heterogenety and exponential distribution of active sites and their energies[58], which is commonly presented as follow:

$$q_e = K_F C_e^{1/n} \quad (4)$$

The Dubinin-Radushkevich (D-R) model is more general than the former two ones because it does not assume a homogenous surface or constant sorption potential[40], and is expressed as below:

$$\ln q_e = \ln q_m - K\varepsilon^2 \quad (5)$$

$$\varepsilon = RT\ln(1+\frac{1}{C_e}) \quad (6)$$

$$E = \frac{1}{\sqrt{2K}} \quad (7)$$

The Langmuir, Freundlich and D-R parameters for adsorption of AF and AO onto NH_2-MCM-41 are listed in Table 2. The Langmuir and Freundlich isotherm models were found to be well representative. But the values of correlation coefficient (R^2) of the Langmuir model were higher than those of the Freundlich model, thus suggesting better description of the adsorption process by the Langmuir model, adsorption to be monolayer on the heterogeneous surface of adsorbent as well as the existence of constant sorption energy during the experimental periods[59]. It can be seen from the data of Langmuir model in the range of 25-40 ^oC，the maximum adsorption capacities of AF and AO onto NH_2-MCM-41 were up to 140.60 mg/g and 278.38 mg/g respectively, and then dropped with the increase of temperature. Under the same experimental conditions, the maximum adsorption capacity of AO onto NH_2-MCM-41 appeared larger than that of AF, which might be due to that the size of AO is smaller than AF, making the resistance lower for the diffusion of AO into inner porous channels of adsorbent, in turn leading to heavier blocking against the adsorption. Besides, the values of R^2 were all higher than 0.90, and all the values of n were in the range of 1-3 simultaneously, demonstrating that AF and AO are comparatively easy to be adsorbed onto NH_2-MCM-41[60].

What is more, the R^2 values of the D-R model were lower compared to those of the two models above, indicating that the D-R model might not fit well with the

equilibrium experimental data. Seen from Table 2, the mean free energies of adsorption (E) were obtained as 1-5 kJ/mol (< 8 kJ/mol), suggesting that the adsorption processes of AF and AO onto NH_2-MCM-41 are predominantly physical in nature[61, 62].

Table 2 Adsorption isotherm constants for adsorption of AF and AO onto NH_2-MCM-41 at various temperatures in single component systems.

Dyes	Temperature(°C)	Langmuir			Freundlich			D-R			
		q_m	K_L	R^2	K_F	n	R^2	Q_m	K	R^2	E
AF	25	140.5972	0.0576	0.9997	19.4659	2.1663	0.9435	73.1932	0.0886	0.6796	2.375
	30	134.7778	0.0818	0.9997	17.7329	2.1186	0.9312	71.5876	0.1220	0.6759	2.024
	40	133.3332	0.0932	0.9967	14.3521	1.9480	0.9673	69.9587	0.1684	0.6591	1.723
AO	25	278.3832	0.0156	0.9987	9.0240	1.3785	0.9639	88.3829	0.1576	0.7910	1.781
	30	224.5360	0.0251	0.9988	7.2514	1.3280	0.9446	88.3351	0.2185	0.8187	1.513
	40	203.5593	0.0357	0.9958	5.4945	1.2388	0.9065	85.1870	0.2671	0.7692	1.368

3.2.7 Adsorption kinetics

Several kinetic models are available to examine the controlling mechanism of the adsorption process which can be divided into two stages[62]: (1) a rapid adsorption within the first 240 min during which more than 90% of the anionic dye removal was completed, and (2) a slow adsorption thereafter until the equilibrium was reached. In this study, adsorption kinetics were investigated applying four kinetic models: Lagergren's pseudo-first-order, the pseudo-second-order, the Spahn and Schlunder model, and the intraparticle diffusion model.

The pseudo-first-order model equation was used for fitting the adsorption of liquid/solid system based on solid capacity[63], which is expressed as:

$$\log(q_e - q_t) = \log q_e - \frac{k_1}{2.303} t \qquad (8)$$

The pseudo-second-order model was applied to predict the adsorption behavior during the entire adsorption period and is in accordance with the adsorption mechanism of rate-controlling steps. The pseudo-second-order equation[64] based on the equilibrium adsorption is given as:

$$\frac{t}{q_t} = \frac{1}{k_2 q_e^2} + \frac{t}{q_e} \quad (9)$$

In order to describe the outer diffusion process of adsorbates to the surface of the adsorbents from the liquid solution, the Spahn and Schlunder model is usually used[65, 66] whose equation is written as:

$$\ln C_t = \ln C_0 - k_{ext} t \quad (10)$$

The intraparticle diffusion model was applied to investigate whether the adsorption process is controlled by more than one diffusion mechanisms, which is very applicable to the inner diffusion of adsorbates inside the adsorbents. Besides, the rate constants of intraparticle diffusion model at different temperatures were determined through the equation as blow[67]:

$$q_t = k_{p,i} t^{0.5} + C \quad (11)$$

The experimental and calculated parameters of the kinetic equations above are summarized in Table 3, and the results of model fitting are shown in Fig. S5 (ESI). Compared to the Lagergren pseudo-first-order kinetic model, the pseudo-second-order fitted the adsorption data better describing the entire adsorption process and all the values of R^2 were greater than 0.998. Moreover, theoretical q_e values of AF and AO were 45.23 mg/g and 47.09 mg/g respectively, highly close to the experimental data (AF: 45.44 mg/g, AO: 47.45 mg/g).

As to the adsorption of dye molecules onto NH_2-MCM-41, three successive stages might exist[68, 69]: (1) film diffusion: adsorbates penetrated across the liquid film to the surface of adsorbent, (2) intraparticle diffusion: most adsorbates diffuse to the pores inside the adsorbent as the adsorbate molecules bound or anchored with the active adsorption sites on the adsorbent surface, and (3) adsorption: adsorption occurred on the inner surface of the adsorbent. The adsorption rate is usually controlled by the first two stages as a consequence of that the adsorption reaction rate on the sorbent surface is far more than the diffusion rate of the adsorbates. In general, film diffusion dominates in the first stage and intraparticle diffusion plays a decisive role when the entire adsorption is almost completed.

In terms of the Spahn and Schlunder model theory (Fig. S5 c, ESI), the relationship between $\ln C_t$ and t would appear linear on condition that the diffusion process of dye molecules from the aqueous solution to NH_2-MCM-41 has a significant impact on the entire adsorption process. It can be observed from Fig. S5 c (ESI) that obvious linear relationships (R^2=0.9560 for AF, R^2=0.8799 for AO) between $\ln C_t$ and t appeared in the initial 120min and 180min respectively, certifying that liquid film diffusion played a dominant part in the primary stage of adsorption, and time needed for liquid film diffusion were 120min (AF) and 180min (AO) respectively.

The intraparticle diffusion model fitting demonstrates the existence of at least two stages in the intraparticle diffusion process (Fig. S5 d, ESI). Firstly, adsorbates were bound onto the adsorbent surface instantly. Then it was the stage of asymptotic

adsorption controlled by micro-intraparticle diffusion rate. As the intraparticle diffusion rate decreased gradually and eventually approached the equilibrium, the concentration of the remaining dyes in the solution had already become rather low, which constituted the last step. Two straight lines both emerged, standing for the asymptotic adsorption stage and equilibrium state respectively (Fig. S5 d, ESI). What is more, the first stage mentioned above did not show up because of the excessively fast adsorption speed. Table 3 shows that $k_{p,2} > k_{p,3}$, which could be attributed to that the dye molecules bound with the adsorption sites rapidly on adsorbent surface in the initial stage, and as the sites approached saturation, dyes started to diffuse into inner surface of NH_2-MCM-41 and then anchored to the active sites there. Compared to the first stage, the reaction rate was smaller in the second stage because of the increasing mass transfer resistance. With the proceed of intraparticle diffusion, amount of dye molecules both in the aqueous solution and on the outer surface of NH_2-MCM-41 gradually decreased, and the driving force of intraparticle diffusion dropped at the same time, leading to falling of adsorption rate and final equilibrium state[70].

Table 3 Kinetic parameters for adsorption of AF and AO onto NH_2-MCM-41 in single component systems.

Dyes	Pseudo-first-order kinetic model			Pseudo-second-order kinetic model			Spahn and Schlunder model			Intraparticle diffusion model		
	k_1	q_e	R^2	k_2	q_e	R^2	k_1	q_e	R^2	k_2	q_e	R^2
AF	0.0172	3.0027	0.9957	0.0237	45.2318	0.9991	0.0172	3.0027	0.9957	0.0237	45.2318	0.9991
AO	0.0102	2.8001	0.9927	0.0993	47.0850	0.9988	0.0102	2.8001	0.9927	0.0993	47.0850	0.9988

3.2.8 Adsorption thermodynamics

In order to investigate the thermodynamic behavior of AF and AO adsorption by

NH_2-MCM-41, parameters such as Gibbs free energy change (ΔG^o), enthalpy (ΔH^o) and entropy (ΔS^o) were calculated according to equations as follows[40]:

$$K_0 = \frac{C_{ad}}{C_e} \tag{12}$$

$$\Delta G^0 = -RT \ln K_0 \tag{13}$$

$$\ln K_0 = \frac{\Delta S^o}{R} - \frac{\Delta H^o}{RT} \tag{14}$$

The thermodynamic parameters for adsorption of AF and AO at different temperatures are listed in Table 4. As we can see from Table 4, the negative ΔG^o and ΔH^o values existed at conditions of various concentrations of dyes and temperatures, indicating that it was thermodynamically feasible, spontaneous and exothermic for the adsorption of AF and AO onto NH_2-MCM-41. The increase of ΔG^o values with rising temperature demonstrated a negative influence of temperature on the adsorption reaction. Moreover, negative ΔS^o values indicated a reduction of randomness at the solid-liquid interface during the adsorption process[71]. Furthermore, the results of adsorption thermodynamics coincided well with those with equilibrium isotherms in this work, and the optimal reaction temperature was 25 °C.

Table 4 Thermodynamic parameters for adsorption of AF and AO onto NH_2-MCM-4 at various temperatures in single component systems.

Dyes	C_0 (mg/L)	ΔH^o (kJ/mol)	ΔS^o (J/mol·K)	ΔG^o (kJ/mol)		
				25 °C	30 °C	40 °C
AF	100	-25.212	-64.719	-5.948	-5.290	-4.967
	150	-22.333	-56.713	-5.414	-5.025	-4.832
	200	-19.162	-47.334	-5.217	-4.775	-4.605
AO	100	-24.287	-60.628	-6.903	-6.713	-6.181
	150	-11.540	-21.629	-6.141	-6.040	-5.267
	200	-21.451	-48.748	-5.127	-4.935	-4.788

3.3 Adsorption in binary component systems

During the past decades, many different kinds of adsorbents have been applied for adsorptive removal of anionic organic dyes from aqueous solutions, which are mostly investigated in single systems. However, more than one dye contaminants exist in the effluent discharged from various industries, which makes it practically meaningful to carry out a research into the adsorption performance of the multi-solute systems[72]. Therefore, we continue to report the adsorption isotherms and kinetics of the binary component systems of AF and AO onto NH_2-MCM-41 at 25 ^oC, pH 2.0 and adsorbent dosage 2.0 g/L in this work.

3.3.1 Adsorption equilibrium isotherms in binary component systems

The Langmuir and Freundlich isotherm models were applied to fit the experimental data of the binary component systems, and the graphs and relevant parameters were presented in Fig. 7 and Table S1 (ESI) , which expatiated that the Langmuir model fitted better compared to the Freundlich model in terms of R^2 values (Table S1, ESI), demonstrating that the former one was more suitable for describing the equilibrium isotherms for adsorption of anionic dyes in the binary component systems, that is, the adsorbed anionic dye molecules were arranged on the available active sites in the form of mono-molecules. By comparing the results in Table 2 and Table S1 (ESI), it is clear that the adsorption removal of the anionic dyes was reduced in the binary component systems since the maximum adsorption capacity of AF and AO decreased form 140.5972mg/g and 278.3832mg/g to 75.4620mg/g and 75.8369mg/g respectively,

which suggested the competitive adsorption between AF and AO dyes.

As a fact that the amount of adsorbent in the aqueous solution was finite, the same-genre anionic dyes AF and AO would be involved in the competition for available adsorption sites on the surface of the adsorbent. The adsorption capacity of each component in the binary systems is frequently less than that of the single component systems, while different decline degrees of adsorption capacity might occur in terms of various kinds of dyes[73].

Furthermore, as a result of that distinctions of the dye molecular structure and size, competitive ability for adsorption sites and adsorption capacity of diverse kinds of dyes may differ[74]. AO with smaller size will mainly defuse into inner spaces of adsorbent easier leading to higher adsorption capacity, hence making AO preponderant in the binary component systems.

3.3.2 Adsorption kinetics in binary component systems

Fig. 8 showed that both the adsorption capacity of AO and AF increased with time until the state of equilibrium was reached in the binary component systems with the same initial dye concentration 100mg/L. Whereas the adsorptive removal percentage of each dye dropped in the binary systems compared to those in the single systems, in conformity with the results of the equilibrium isotherms in the binary component systems. Besides, the decline degree of AF removal percentage appeared higher than that of AO removal in the binary systems, which might be due to competitive adsorption between the same-type anionic dyes in the mixture aqueous solution[48]. In

this present work, the pseudo-first-order, pseudo-second-order, Spahn and Schlunder and intraparticle diffusion models were adopted to fit the kinetic data of the experiment, and the kinetic parameters are summarized in Table S2 (ESI).

The adsorption kinetics could be better described by the pseudo-second-order model with higher R^2 values ($R^2>0.994$) compared to those ($R^2>0.950$) of the pseudo-second-order model (Table S2, ESI), close to ideal values in all cases, and in consistent with the results of adsorption kinetics in single component systems, which also suggested that the dye adsorption onto NH_2-MCM-41 would be altered in binary component systems[75]. In binary component systems, the theoretical q_e values of AF and AO were respectively 18.9268mg/g and 20.8688mg/g, while the corresponding values in single systems were up to 45.2318mg/g and 47.0850mg/g, which could be attributed to competition for adsorption in the mixture solution[48].

It can be seen from Fig. 8 c that the linear relations between $\ln C_t$ and t of both the two anionic dyes could be ascribed to the comparatively higher impact of the diffusion procedure from the liquid phase to the surface of adsorbent of the whole adsorption process in binary component systems. Additionally, two straight lines appeared after the intraparticle diffusion kinetic fitting (Fig. 8 d), suggesting the probable existence of at least two steps influencing the rate of adsorption in binary component systems. By comparing the parameters between the binary and single component systems from Table 3 and Table S2 (ESI), the $k_{p,2}$ value of AF decreased from 4.8327 mg/(g·min$^{0.5}$) to 1.3036 mg/(g·min$^{0.5}$), and from 4.1846 mg/(g·min$^{0.5}$) to 0.9559 mg/(g·min$^{0.5}$) for AO. However, all of the $k_{p,3}$ values became higher in

comparison with those of the single systems, which could be due to mutual influence of the competitive adsorption and the concentrations of dyes in the multi-solute aqueous solution[76].

4. Conclusions

On the basis of results in this work, NH_2-MCM-4 prepared was a promising adsorbent material for removing anionic dyes with sulfonic groups from aqueous solutions. Various experimental parameters including solution pH, adsorbent dosage, contact time, initial dye concentration and temperature had influences on adsorption of AF and AO using NH_2-MCM-4. It was found that the adsorption isotherm data fitted well with the Langmuir and D-R models, suggesting the adsorption to be monolayer and physical in nature. The kinetic processes of AF and AO adsorption by NH_2-MCM-4 could be preferably described by the pseudo-second-order kinetic model as well as the Spahn and Schlunder model. Besides, the intraparticle diffusion model indicated the controlling nature of film diffusion followed by intraparticle diffusion. In addition, the thermodynamic calculations demonstrated the feasible, spontaneous and exothermic nature of the adsorption reaction. For binary component systems, AF and AO exhibited competitive adsorption onto NH_2-MCM-41, and the adsorption capacities was reduced at pH 2.0, 25 ^oC in comparison with those of the corresponding single component systems for AF and AO. The experimental data were fairly better fitted by the Langmuir isotherm and the pseudo-second-order kinetic models from adsorption equilibrium isotherm and kinetic studies both in single and binary component

systems.

5. Definitions

C_e liquid phase dye concentration at equilibrium ($mg \cdot L^{-1}$)

C_0 initial liquid concentrations of dye ($mg \cdot L^{-1}$)

C_t liquid concentrations of dye at any time($mg \cdot L^{-1}$)

C_{ad} liquid concentrations of reduced dye ($mg \cdot L^{-1}$)

k_1 equilibrium rate constant of pseudo-first-order adsorption (min^{-1})

k_2 equilibrium rate constant of pseudo-second-order adsorption ($g\ (mg \cdot min)^{-1}$)

k_{ext} external diffusion constant (min^{-1})

$k_{p,i}$ the intraparticle diffusion rate parameters of different stages

K the constant giving the mean free energy of adsorption per molecular of the adsorbate

K_0 the equilibrium constant

K_F Freundlich constant indicative of the relative adsorption capacity of the sorbent ($mg \cdot g^{-1}$)

K_L Langmuir sorption constant ($L \cdot mg^{-1}$)

q_e amount of solute adsorbed per unit weight of the adsorbent at equilibrium ($mg \cdot g^{-1}$)

q_m maximum adsorption capacity of the adsorbent ($mg \cdot g^{-1}$)

q_t amount of solute adsorbed per unit weight of the adsorbent at any time ($mg \cdot g^{-1}$)

R gas constant ($8.314\ J\ (mol \cdot K)^{-1}$)

R^2 correlation coefficient

E mean free energy of sorption (kJ·mol^{-1})

ε Polanyi potential

n Freundlich constant indicative of the intensity of adsorption

T absolute temperature (^{o}C)

t time (min)

M the weight of the dyes used (g)

V the volume of the aqueous solution (L)

Acknowledgements

The authors acknowledge much help from Huang Xin. Besides, the authors are thankful to Hohai University for financial and technical assistance during this work.

References

1. P. Grau, Water Sci. Technol., 1991, 24, 97-103.
2. V. Vinod and T. Anirudhan, Water, Air, Soil Pollut., 2003, 150, 193-217.
3. G. Crini and P.-M. Badot, Prog. Polym. Sci., 2008, 33, 399-447.
4. A. Mittal, J. Mittal, A. Malviya and V. Gupta, J. Colloid Interface Sci., 2009, 340, 16-26.
5. A. Mittal, J. Mittal, A. Malviya and V. Gupta, J. Colloid Interface Sci., 2010, 344, 497-507.
6. T. O'mahony, E. Guibal and J. Tobin, Enzyme Microb. Technol., 2002, 31, 456-463.
7. A. S. Özcan and A. Özcan, J. Colloid Interface Sci., 2004, 276, 39-46.
8. A. Mittal, D. Kaur, A. Malviya, J. Mittal and V. Gupta, J. Colloid Interface Sci., 2009, 337, 345-354.
9. A. Mittal, J. Mittal, A. Malviya, D. Kaur and V. Gupta, J. Colloid Interface Sci., 2010, 342, 518-527.
10. A. El Sikaily, A. Khaled, A. E. Nemr and O. Abdelwahab, Chem. Ecol., 2006, 22, 149-157.
11. M. Kornaros and G. Lyberatos, J. Hazard. Mater., 2006, 136, 95-102.
12. Y. Hu, T. Guo, X. Ye, Q. Li, M. Guo, H. Liu and Z. Wu, Chem. Eng. J., 2013, 228, 392-397.
13. A. M. Faouzi, B. Nasr and G. Abdellatif, Dyes Pigm., 2007, 73, 86-89.
14. S. Karthikeyan, V. Gupta, R. Boopathy, A. Titus and G. Sekaran, J. Mol. Liq., 2012, 173, 153-163.
15. J. Labanda, J. Sabaté and J. Llorens, J. Membr. Sci., 2009, 340, 234-240.
16. D. S. Orlov, Soil chemistry, AA Balkema Publishers, 1992.
17. M. Oladipo, I. Bello, D. Adeoye, K. Abdulsalam and A. Giwa, Adv. Eng. Biology, 2013, 7, 3311-3327.
18. V. K. Gupta, I. Ali, T. A. Saleh, A. Nayak and S. Agarwal, RSC Adv., 2012, 2, 6380-6388.
19. H. S. Rai, M. S. Bhattacharyya, J. Singh, T. Bansal, P. Vats and U. Banerjee, Crit. Rev. Environ. Sci. Technol., 2005, 35, 219-238.
20. V. K. Gupta, R. Jain, A. Nayak, S. Agarwal and M. Shrivastava, Mater. Sci. Eng., C, 2011, 31, 1062-1067.
21. T. A. Saleh and V. K. Gupta, J. Colloid Interface Sci., 2012, 371, 101-106.
22. V. K. Gupta, R. Jain, A. Mittal, T. A. Saleh, A. Nayak, S. Agarwal and S. Sikarwar, Mater. Sci. Eng., C, 2012, 32, 12-17.
23. H. Khani, M. K. Rofouei, P. Arab, V. K. Gupta and Z. Vafaei, J. Hazard. Mater., 2010, 183, 402-409.
24. V. Gupta, S. Srivastava, D. Mohan and S. Sharma, Waste Manage., 1997, 17, 517-522.
25. S. Allen and B. Koumanova, J. Univ. Chem. Technol. Metallurgy, 2005, 40, 175-192.
26. V. K. Gupta, S. Agarwal and T. A. Saleh, J. Hazard. Mater., 2011, 185, 17-23.
27. T. A. Saleh and V. K. Gupta, Environ. Sci. Pollut. Res., 2012, 19, 1224-1228.
28. A. Jain, V. Gupta, A. Bhatnagar and Suhas, Sep. Sci. Technol., 2003, 38, 463-481.
29. V. Gupta and A. Nayak, Chem. Eng. J., 2012, 180, 81-90.
30. L.-C. Juang, C.-C. Wang and C.-K. Lee, Chemosphere, 2006, 64, 1920-1928.
31. X. Zhao, G. Lu and X. Hu, Microporous Mesoporous Mater., 2000, 41, 37-47.
32. A. Vinu, K. Z. Hossain and K. Ariga, J. Nanosci. Nanotechnol., 2005, 5, 347-371.
33. B. Boukoussa, R. Hamacha, A. Morsli and A. Bengueddach, Arabian J. Chem, 2013.
34. K. Parida and D. Rath, J. Mol. Catal. A: Chem., 2009, 310, 93-100.

35. H. Yoshitake, T. Yokoi and T. Tatsumi, Chem. Mater., 2003, 15, 1713-1721.
36. A. Heidari, H. Younesi and Z. Mehraban, Chem. Eng. J., 2009, 153, 70-79.
37. C.-K. Lee, S.-S. Liu, L.-C. Juang, C.-C. Wang, K.-S. Lin and M.-D. Lyu, J. Hazard. Mater., 2007, 147, 997-1005.
38. J. R. Sohn, S. J. DeCanio, J. H. Lunsford and D. J. O'Donnell, Zeolites, 1986, 6, 225-227.
39. V. Umamaheswari, M. Palanichamy and V. Murugesan, J. Catal., 2002, 210, 367-374.
40. J. Cao, Y. Wu, Y. Jin, P. Yilihan and W. Huang, J. Hazard. Mater., 2014, 45, 860-868.
41. S. Muto and H. Imai, Microporous Mesoporous Mater., 2006, 95, 200-205.
42. M. P. Elizalde-González and V. Hernández-Montoya, Bioresour. Technol., 2009, 100, 2111-2117.
43. F. Doulati Ardejani, K. Badii, N. Y. Limaee, S. Z. Shafaei and A. Mirhabibi, J. Hazard. Mater., 2008, 151, 730-737.
44. R. Gong, Y. Ding, M. Li, C. Yang, H. Liu and Y. Sun, Dyes Pigm., 2005, 64, 187-192.
45. K. Santhy and P. Selvapathy, Bioresour. Technol., 2006, 97, 1329-1336.
46. C. Namasivayam and D. Kavitha, Dyes Pigm., 2002, 54, 47-58.
47. Y. Fu and T. Viraraghavan, Adv. Environ. Res., 2002, 7, 239-247.
48. R. Saad, K. Belkacemi and S. Hamoudi, J. Colloid Interface Sci., 2007, 311, 375-381.
49. T. Yokoi, T. Tatsumi and H. Yoshitake, J. Colloid Interface Sci., 2004, 274, 451-457.
50. M. M. Mohamed, J. Colloid Interface Sci., 2004, 272, 28-34.
51. M. Anbia and S. Salehi, Dyes Pigm., 2012, 94, 1-9.
52. A. E. Nemr, O. Abdelwahab, A. El-Sikaily and A. Khaled, J. Hazard. Mater., 2009, 161, 102-110.
53. G. Moussavi and R. Khosravi, Chem. Eng. Res. Des., 2011, 89, 2182-2189.
54. D. Sun, X. Zhang, Y. Wu and X. Liu, J. Hazard. Mater., 2010, 181, 335-342.
55. P. H. Pacheco, R. Olsina, G. Polla, L. D. Martinez and P. Smichowski, Microchem. J., 2009, 91, 159-164.
56. A. Sarı and M. Tuzen, J. Hazard. Mater., 2009, 164, 1004-1011.
57. C. Almeida, N. Debacher, A. Downs, L. Cottet and C. Mello, J. Colloid Interface Sci., 2009, 332, 46-53.
58. S. Kocaoba, J. Hazard. Mater., 2007, 147, 488-496.
59. R. A. Anayurt, A. Sari and M. Tuzen, Chem. Eng. J., 2009, 151, 255-261.
60. Y. Wu, S. Feng, B. Li and X. Mi, World J. Microbiol. Biotechnol., 2010, 26, 249-256.
61. S. Tunali, T. Akar, A. S. Özcan, I. Kiran and A. Özcan, Sep. Purif. Technol., 2006, 47, 105-112.
62. K.-Y. Shin, J.-Y. Hong and J. Jang, J. Hazard. Mater., 2011, 190, 36-44.
63. Y. Wu, J. Cao, P. Yilihan, Y. Jin, Y. Wen and J. Zhou, RSC Adv., 2013, 3, 10745-10753.
64. Y.-S. Ho and G. McKay, Water Res., 2000, 34, 735-742.
65. H. Spahn and E. Schlünder, Chem. Eng. Sci., 1975, 30, 529-537.
66. W. Fritz, W. Merk and E. Schluender, Chem. Eng. Sci., 1981, 36, 743-757.
67. A. Salima, B. Benaouda, B. Noureddine and L. Duclaux, Water Res., 2013, 47, 3375-3388.
68. D. Duranoğlu, A. W. Trochimczuk and U. Beker, Chem. Eng. J., 2012, 187, 193-202.
69. A. B. Albadarin, C. Mangwandi, A. a. H. Al-Muhtaseb, G. M. Walker, S. J. Allen and M. N. Ahmad, Chem. Eng. J., 2012, 179, 193-202.
70. R. D. Letterman, Water quality and treatment: a handbook of community water supplies,

McGraw-hill New York, 1999.
71. M. Jain, V. Garg and K. Kadirvelu, J. Hazard. Mater., 2009, 162, 365-372.
72. S. Eftekhari, A. Habibi-Yangjeh and S. Sohrabnezhad, J. Hazard. Mater., 2010, 178, 349-355.
73. Y. Al-Degs, M. Khraisheh, S. Allen, M. Ahmad and G. Walker, Chem. Eng. J., 2007, 128, 163-167.
74. Y. Wu, L. Jiang, Y. Wen, J. Zhou and S. Feng, Environ. Sci. Pollut. Res., 2012, 19, 510-521.
75. S. Wang, C. W. Ng, W. Wang, Q. Li and Z. Hao, Chem. Eng. J., 2012, 197, 34-40.
76. M.-S. Chiou and G.-S. Chuang, Chemosphere, 2006, 62, 731-740.

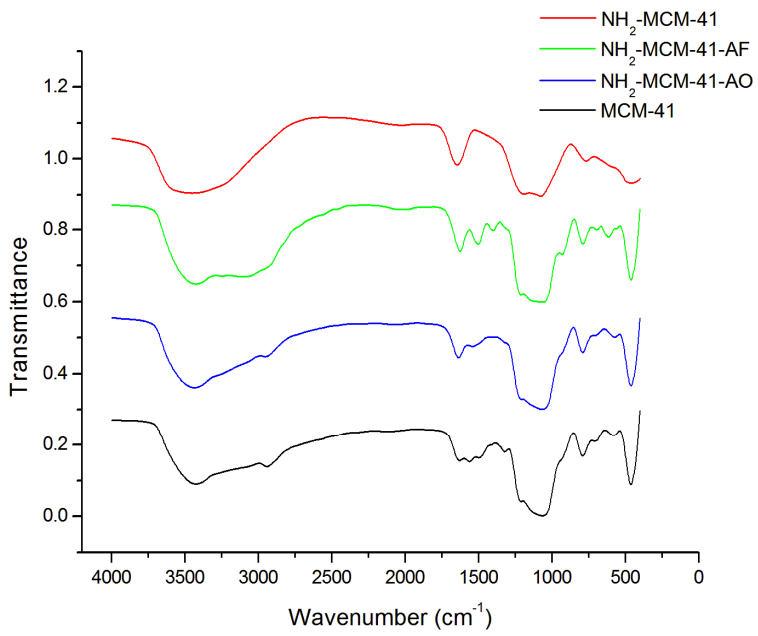

Fig. 1 FTIR spectra of MCM-41, NH_2-MCM-41, NH_2-MCM-41-AF and NH_2-MCM-41-AO.

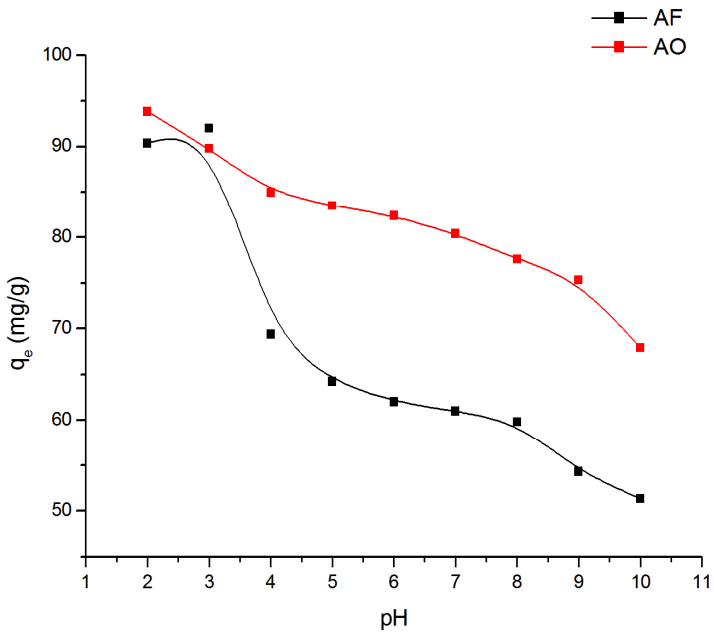

Fig. 2 Effect of pH on adsorption of AF and AO in single component systems. a: AF, b: AO. (Conditions: 25 ^{o}C, dye concentration 100mg/L, NH_2-MCM-41 dosage 1.0 g/L.)

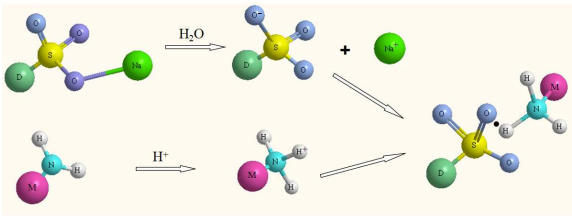

Fig. 3 Schematic illustration of the adsorption reactions in aqueous solution. Where D and M represent the other fractions in the two-kind dye molecules and NH_2-MCM-41 respectively.

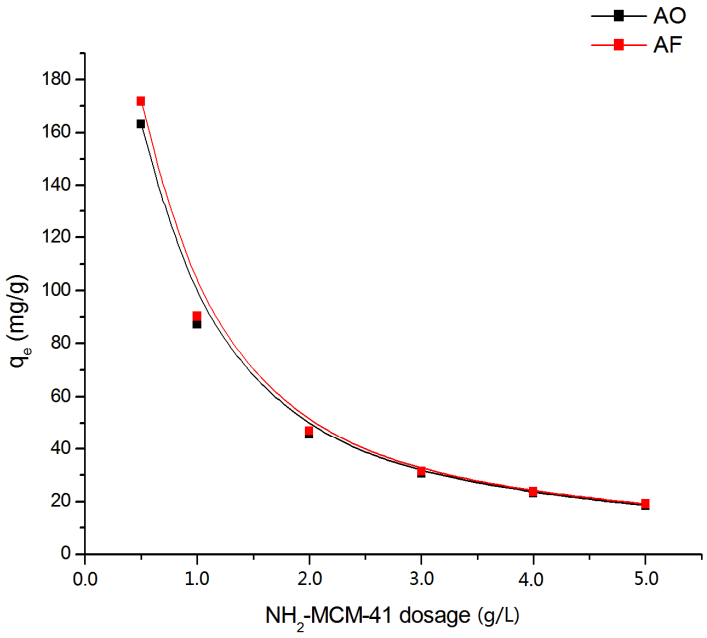

Fig. 4 Effect of NH_2-MCM-41 dosage on adsorption of anionic dyes in single component systems. a: AF, b: AO. (Conditions: pH 3.0 for AF and 2.0 for AO, 25 ^oC, dye concentration 100mg/L.)

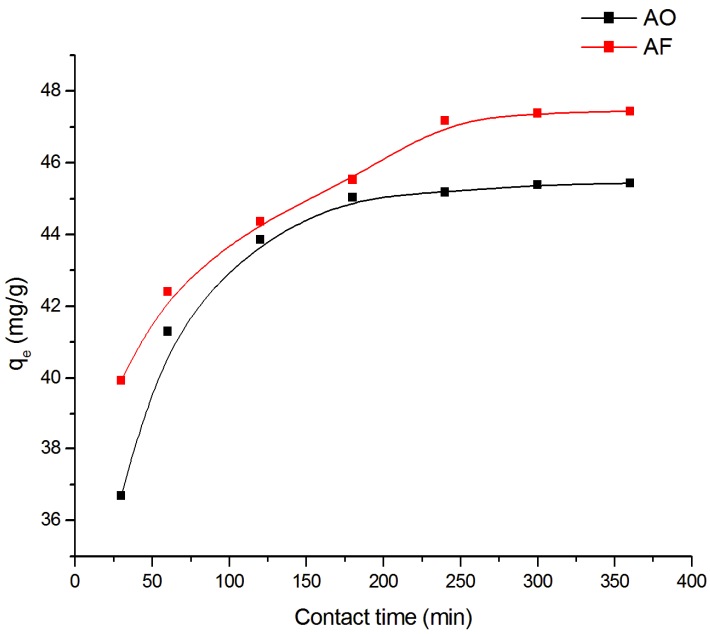

Fig. 5 Effect of contact time on adsorption of anionic dyes in single component systems. a: AF, b: AO. (Conditions: pH 3.0 for AF and 2.0 for AO, 25^oC, dye concentration 100mg/L, NH_2-MCM-41 dosage 2.0 g/L.)

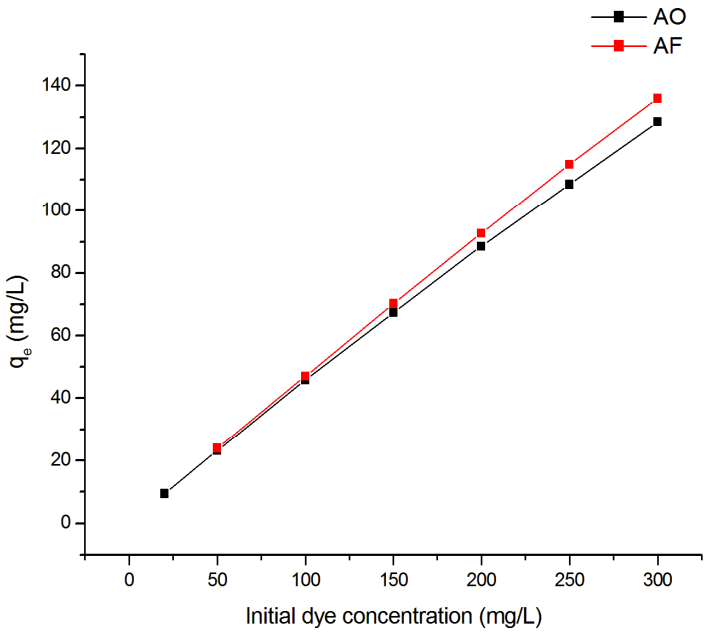

Fig. 6 Effect of initial dye concentration on adsorption of anionic dyes in single component systems. a: AF, b: AO. (Conditions: pH 3.0 for AF and 2.0 for AO, 25 ^{o}C, NH_2-MCM-41 dosage 2.0 g/L.)

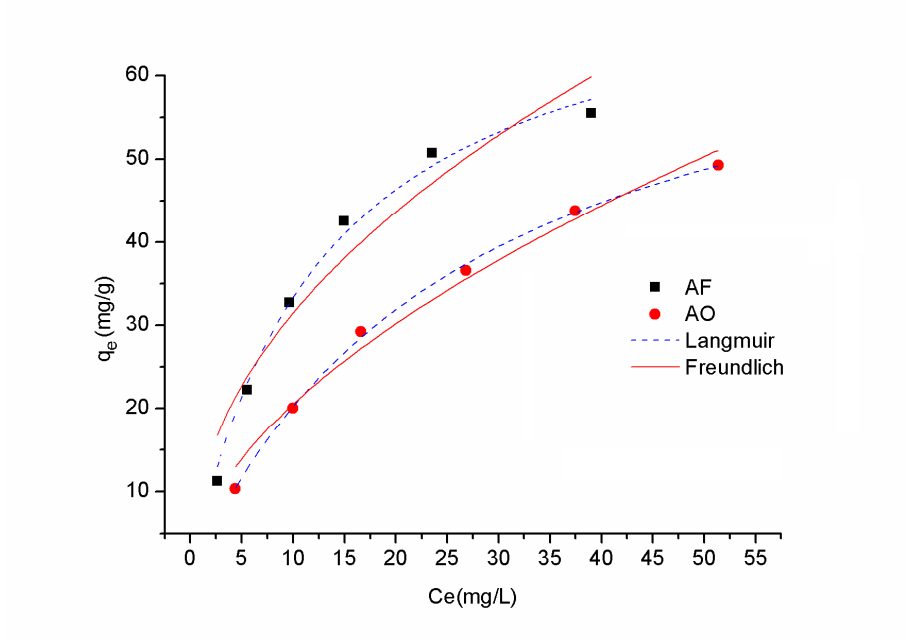

Fig. 7 Adsorption equilibrium isotherms of AF and AF onto NH_2-MCM-41 in binary component systems. a: Langmuir isotherm model fitting, b: Freundlich isotherm model fitting. (Conditions: pH 2.0, 25 ^oC, NH_2-MCM-41 dosage 2.0 g/L.)

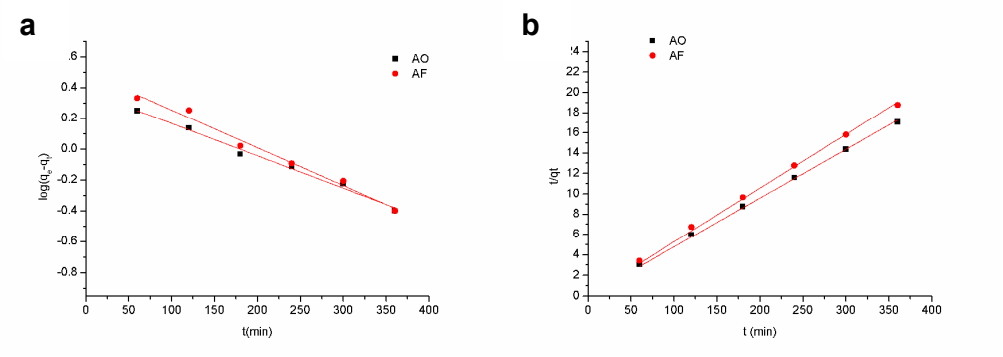

a: Pseudo-first-order kinetic model fitting b: Pseudo-second-order kinetic model fitting

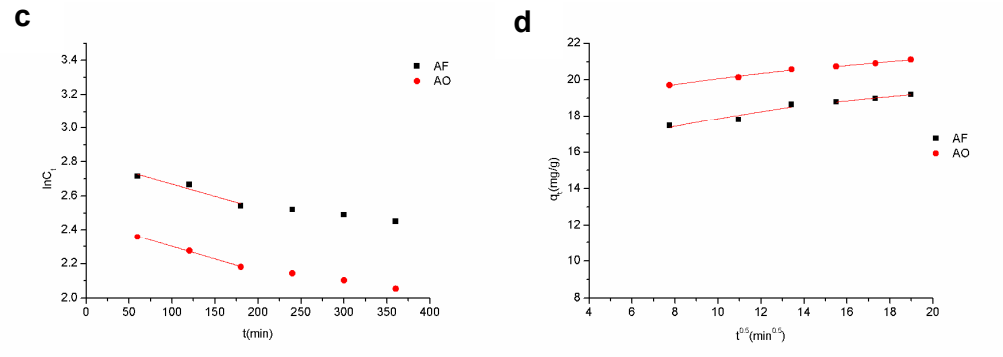

c: Spahn and Schlunder model fitting d: Intraparticle diffusion model fitting

Fig. 8 Adsorption kinetics of AF and AO onto NH_2-MCM-41 in binary component systems. a: Pseudo-first-order kinetic model fitting, b: Pseudo-second-order kinetic model fitting, c: Spahn and Schlunder model fitting, d: Intraparticle diffusion model fitting. (Conditions: pH 2.0, 25 ^oC, NH_2-MCM-41 dosage 2.0 g/L.)